



ELSEVIER

Journal of Photochemistry and Photobiology A: Chemistry 101 (1996) 189–196

Journal of
PHOTOCHEMISTRY
AND
PHOTOBIOLOGY
A: CHEMISTRY

Photochemical intramolecular γ -hydrogen abstraction in a ketone and an alkene and the role of tunneling of hydrogen

V. Sreedhara Rao, A.K. Chandra

Department of Inorganic and Physical Chemistry, Indian Institute of Science, Bangalore 560 012, India

Received 1 April 1996; accepted 28 May 1996

Abstract

Intramolecular γ -hydrogen abstraction reactions were examined in pentane-2-one and 2-methyl-1-pentene in their lowest triplet states using the AM1 semi-empirical molecular orbital method with the complete geometry optimization in the unrestricted Hartree–Fock frame. The results reveal that the oxygen atom of the carbonyl group and the end carbon atom of the olefinic bond acquire high free valence and spin density indices in their respective lowest triplet states, leading to abstraction of hydrogen from the γ -position relative to the carbonyl and olefinic bonds. The theoretical energy profiles fit with a polynomial and the probability of tunneling of hydrogen was estimated by the WKB (Wentzel, Kramer and Brillouin) method. The results, after thermal averaging of the rate constants, reveal that tunneling of hydrogen is significant at room temperature.

Keywords: γ -Hydrogen abstraction; Hydrogen tunnelling; Alkene; Ketone

1. Introduction

Photochemical intramolecular γ -hydrogen transfer reactions by carbonyl compounds have been studied extensively [1–3]. However, intramolecular γ -hydrogen abstraction reactions of olefins are less well documented. There are a few reports [4–7] which indicate that hydrogen transfer reactions occur in the photochemistry of alkenes. For example, 1:5 hydrogen transfer reactions of an α -alkyl styrene in its triplet state were observed with very low quantum yield. Padwa et al. [8] reported several examples of the Norrish type II photoreaction in substituted cyclopropenes where quantum yields are high. The triplet ($\pi\pi^*$) states of some substituted cyclopropenes which possess γ -hydrogen undergo an intramolecular hydrogen transfer reaction via a six-membered ring transition state by a mechanism analogous to the well known Norrish type II reaction of carbonyl compounds. This is possible because triplet-state lifetimes of cyclopropenes are 100 times greater than those of the related phenyl alkenes. Padwa and Terry [9] noted that when the migrating hydrogen is replaced by deuterium, the isotope effect (i.e. k_H/k_D where k_H and k_D are the specific rate constants for hydrogen and deuterium transfer respectively) is 3.0. An observation of a low value of the isotope effect may suggest that the primary step in the Norrish type II process is an electron transfer rather than one-step hydrogen transfer. The deuterium isotope effect

in the intramolecular γ -hydrogen abstraction of the triplet state of ketone is not reported. There are some reports [10] of the isotope effect on the intermolecular processes by the triplet states of ketones. For example, the deuterium isotope effect on the reaction of acetone (${}^3n\pi^*$) with methane is 3.7 at room temperature. Grellmann and coworkers [11,12] studied the photo-enolization process of 5:8 dimethyl-1-tetralone. This process involves 1:5 hydrogen transfer on the lowest triplet state surface. They concluded that the hydrogen transfer in this process is primarily controlled by tunneling around room temperatures. More recently, a report [13] appeared on the enolization of 1:4 dimethyl anthrone and suggested that at low temperature (30 K) deuterium tunneling dominates. However, it is not clear whether the hydrogen transfer takes place in the singlet or triplet state surface. Similar experiments were not reported for the intramolecular γ -hydrogen abstraction process by ketones at different temperatures monitoring the other photophysical processes. Encina and Lissi [14] reported the Arrhenius parameters for γ -hydrogen abstraction by the lowest triplet state of pentane-2-one in polar medium. They assumed that intersystem crossing, photoreactions with solvent and the type I photocleavage processes were negligible. Wagner et al. [15] reported the type II process for phenyl ketones from the triplet states and observed that the deuteration at the γ -position produced no change in quantum yield but increased the triplet lifetime.

Recently, we [16] examined the role of tunneling of hydrogen in the photo-enolization of a ketone with a hydrogen atom in the γ -position relative to the carbonyl group. Our results reveal that tunneling of hydrogen is significant in the enolization process which involves 1:5 hydrogen transfer, in the temperature range 80–350 K. The object of this investigation is to make a comparative study of the Norrish type II processes in pentane-2-one and 2-methyl-1-pentene and also to examine the role of tunneling of hydrogen. Fig. 1 shows the equilibrium structures of pentane-2-one (**IA**) and pentane-2-ene (**IB**) in their respective lowest triplet ($n\pi^*$) and ($\pi\pi^*$) states. Intramolecular hydrogen abstraction in these two systems involves 1:5 hydrogen transfer and the formation of six-membered ring transition states which are almost strain free. In order to attain the cyclic arrangement, the molecules **IA** and **IB** must rearrange from the stable conformation to a nearly cyclic conformation by internal rotation. If the barrier to internal rotation is very large, hydrogen transfer cannot take place within the lifetime of the triplet states. Scheffer [17] suggested that unless the abstractable hydrogen comes within 2.7–3.0 Å of the carbonyl oxygen, reaction cannot occur. In our earlier investigations [3,18,19], we observed that the abstractable hydrogen is first brought close to the carbonyl oxygen by internal rotation around the β -bond relative to the carbonyl group. This requires a small barrier from the equilibrium conformation ($\alpha \sim 180^\circ$, $\beta \sim 180^\circ$, $\gamma \sim 180^\circ$) where α , β and γ are the dihedral angles shown in Fig. 1. In order to compare the relative rates of the Norrish type II process in a ketone and in a comparable alkene, we maintain the same level of calculations. We employed the AM1 method [20] in the unrestricted Hartree–Fock (UHF) frame which is preferable, as this allows different orbitals for each electron, for treatment of the open-shell systems. It should be noted here that for treatment of pentane-2-one we employed the MINDO/3 method in Ref. [3].

2. Computational method

We employed the AM1 method in the UHF frame and calculations were performed using the MOPAC [21] program. Calculations were performed for various values of α ,

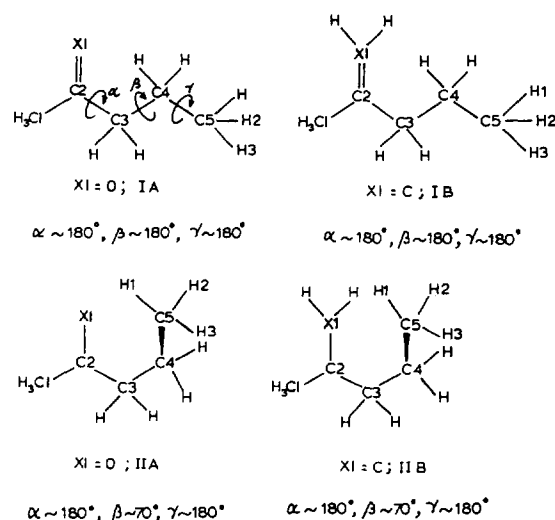


Fig. 1. Two conformers of pentane-2-one and 2-methyl-1-pentene, each defined by the dihedral angles α , β and γ .

β and γ , optimizing all the geometrical parameters. Since the Norrish type II process takes place in the lowest triplet state, we examined the energetics of the conformational changes in the triplet state by the AM1 method. Fig. 2 shows the variation of energy change ΔE relative to the conformer **I** with β , while α is optimized. Using the conformers **IIA** and **IIB** for the ketone and alkene respectively, as reactants, we reduced the X1–H1 distance and the BFGS (Broyden, Fletcher, Goldfarb, Shanno) optimization procedure [21] was carried out until 1:4 biradicals were obtained. This was identified by the two highest singly occupied molecular orbitals localized on C5 and C2 (Fig. 1). Transition-state structures were characterized by only one negative eigenvalue of the force constant matrix. We considered the hydrogen-transfer reaction along the minimum energy path (MEP) on the lowest triplet state surfaces of the ketone (${}^3n\pi^*$) and alkene (${}^3\pi\pi^*$) as a function of the X1–H1 distance while optimizing the remaining geometrical parameters. The magnitude of the imaginary frequencies is 2148i cm^{-1} for pentane-2-one and 2068i cm^{-1} for 2-methyl-1-pentene. The normal coordinate analysis shows that the eigenvectors corresponding to these imaginary frequencies are the asymmetric stretch of the non-linear triatomic systems X1–H1–C5. Hence, the reaction coordinate near the transition state could be taken as $x = R_{\text{C5-H1}} - R_{\text{X1-H1}}$

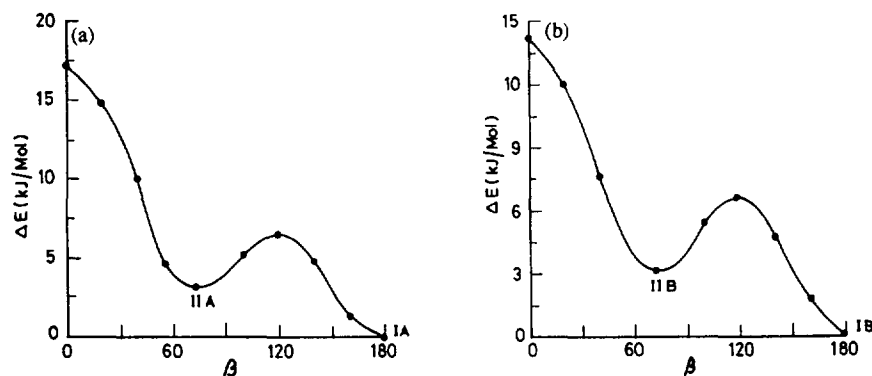


Fig. 2. ΔE vs. β plots for ketone (a) and alkene (b), in their lowest triplet states while α is optimized.

where R_{C5-H1} and R_{X1-H1} are respectively the lengths of the C5–H1 and X1–H1 bonds.

For calculation of bond-orders, free valences and spin densities, we follow Mayer's formalism [22–24]. According to Mayer, the bond-order between atoms A and B in a molecule is given as

$$B_{AB} = 2 \sum_{\mu \in A} \sum_{\nu \in B} (P^\alpha S)_{\mu\nu} (P^\alpha S)_{\nu\mu} + (P^\beta S)_{\mu\nu} (P^\beta S)_{\nu\mu} \quad (1)$$

where S is the overlap matrix, P^α and P^β are the density matrices for α and β spins respectively. The valence on atom A is given as

$$V_A = F_A + \sum_{B \neq A} B_{AB} \quad (2)$$

where F_A is the free valence on atom A which is given by

$$F_A = \sum_{\mu, \nu \in A} (P^s S)_{\mu\nu} (P^s S)_{\nu\mu} \quad (3)$$

where $P^s = P^\alpha - P^\beta$.

The spin density on atom A is defined as

$$T_A = \sum_{\mu \in A} (P^s S)_{\mu\mu} \quad (4)$$

In a semi-empirical theory, the overlap matrix S is taken to be the unit diagonal matrix. It can be proved easily that for a migrating hydrogen atom the free valence is equal to the square of the spin density [25].

3. Results

The UHF calculations at the AM1 level reveal that the lowest triplet states of the ketone (**IA**) and the alkene (**IB**) are, respectively, the $n\pi^*$ and $\pi\pi^*$ states. In both cases, excitations are localized on their respective chromophores. In the case of alkene, the p_π -orbital on C1 is rotated by 90° from the previous π -plane as in ethylene. Our calculations reveal that the 1:5 hydrogen transfer in the (${}^3n\pi^*$) state of ketone is exothermic by 65 kJ mol^{-1} while, in the lowest ${}^3\pi\pi^*$ of the alkene, the process is almost thermoneutral. The conformers **IIA** and **IIB** for ketone and alkene are only 3 kJ mol^{-1} above their corresponding conformers **IA** and **IB**. Fig. 3 shows the minimum energy paths (MEP) obtained by intrinsic reaction coordinate calculations for intramolecular hydrogen abstraction processes from conformers **IIA** and **IIB**. The calculations reveal that the optimized structures of the transition states are six-membered slightly puckered rings (Fig. 4). The barriers for hydrogen abstraction are nearly the same for both ketone and alkene. They are approximately 68 kJ mol^{-1} before and approximately 44 kJ mol^{-1} after the zero-point energy corrections. Fig. 4 shows the optimized structures of the reactant (conformer **II**), the corresponding transition state structures and the nascent 1:4 biradicals. Free valences and spin densities on C5, H1, O (or C1) and C2 are indicated in the same figure.

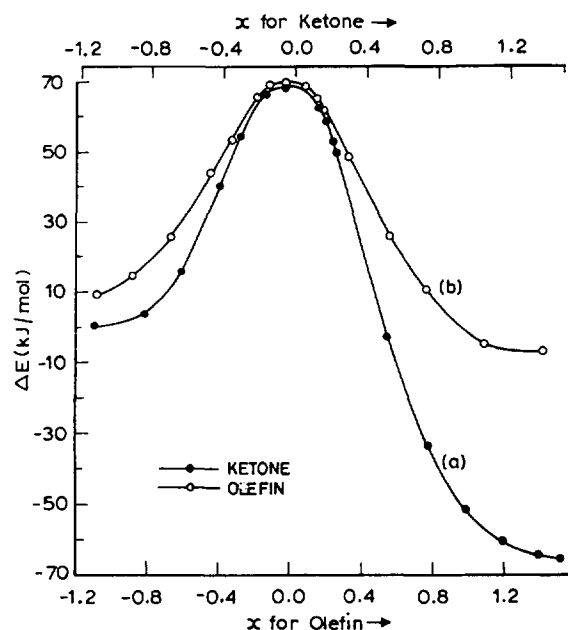


Fig. 3. Curve (a) shows the energy profile for the γ -hydrogen abstraction in ketone. Curve (b) gives the energy profile for the same process in alkene. The energy profiles were obtained by the AM1 (UHF) method.

4. Discussion

If we use the simple Arrhenius equation with the pre-exponential factor of 10^{13} s^{-1} which is the frequency of free internal rotation, a barrier height of 44 kJ mol^{-1} leads to a unimolecular rate constant of 10^5 s^{-1} at 300 K. For pentane-2-one, the rate constant for hydrogen abstraction from the triplet state in hexane has been estimated at $1.3 \times 10^7 \text{ s}^{-1}$ [26]. The observed larger rate constant for the hydrogen transfer process in ketone may be due to the tunneling of hydrogen. No kinetic data are available for any alkene, but according to the transition-state theory, the rate constants for ketone and alkene should be nearly the same.

4.1. Structural and electronic properties of the transition states

Wagner [27] has suggested that the photochemical hydrogen transfer process in ketones occurs via charge-transfer followed by proton transfer. This path is evident in amines but not when triplet ketones are reduced by saturated hydrocarbons. We now examine the structural and electronic characteristics of the transition state for the ketone and alkene. The most important geometrical changes at the transition state are the bond distances r' and r of the newly forming X1–H1 and the breaking C5–H1 bonds respectively. The relative bond distances r'_{rel} and r_{rel} are defined as

$$r'_{\text{rel}} = \frac{r'^*}{r'_e} \quad r_{\text{rel}} = \frac{r^*}{r_e} \quad (5)$$

where r'^* and r^* are the X1–H1 and C5–H1 bond distances in the transition state and r'_e and r_e are the corresponding equilibrium bond lengths in the product and the C5–H1 bond

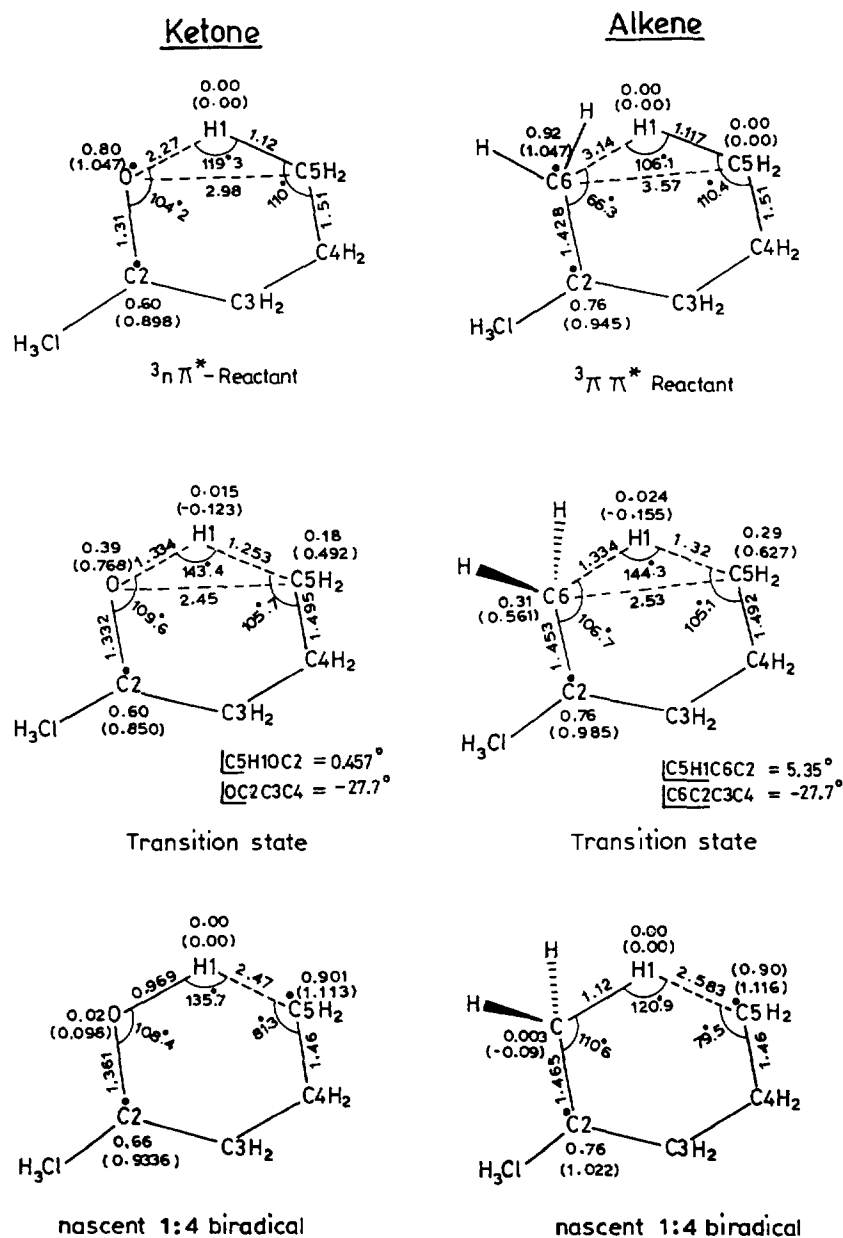


Fig. 4. The optimized structures of the reactants, transition states and the nascent 1:4 biradicals. The numbers in parentheses are spin densities. Free valence indices are shown on the atoms. Bond lengths are given in ångströms.

length in the reactant from which H1 is abstracted. It has been shown that the ratio $r_{\text{rel}}/r'_{\text{rel}}$ is equal to unity for thermoneutral hydrogen transfer reactions [28], but for exothermic reactions this ratio is less than unity, corresponding to more reactant-like transition states. From the optimized bond length data, we find that $r_{\text{rel}}/r'_{\text{rel}}$ is 0.81 for the intramolecular γ -hydrogen transfer process in ketone, which is highly exothermic. However, for the similar process which is nearly thermoneutral in alkene, the ratio $r_{\text{rel}}/r'_{\text{rel}}$ is around 1.0. The results of calculations are therefore internally consistent.

4.2. Radical-like reactivity and free valence (spin density) indices

The results in Fig. 4 indicate that the radical-like reactivity should be more prominent on the C1 atom in 2-methyl-1-

pentene in its lowest ($^3\pi\pi^*$) state than on the O1 atom in pentane-2-one in its lowest ($^3n\pi^*$) state. The reactivity of the ($^3\pi\pi^*$) excited states of olefins towards H-atom abstraction has been observed in intermolecular processes [29], where the rate of H-abstraction is found to be about 10^3 times higher than that from the ($^3n\pi^*$) state of a ketone. Fig. 4 also shows the development of free valence (or spin density) on the migrating hydrogen. Recently, we [25] observed that the development of free valence (or spin density) on the migrating hydrogen atom during the radical-exchange reactions can be used as a criterion for location of the saddle points. Fig. 5 shows the plots of free valence (and spin density) indices of the migrating hydrogen atom as a function of the reaction coordinate x , during the intramolecular hydrogen abstractions. The results show that the saddle points in the energy

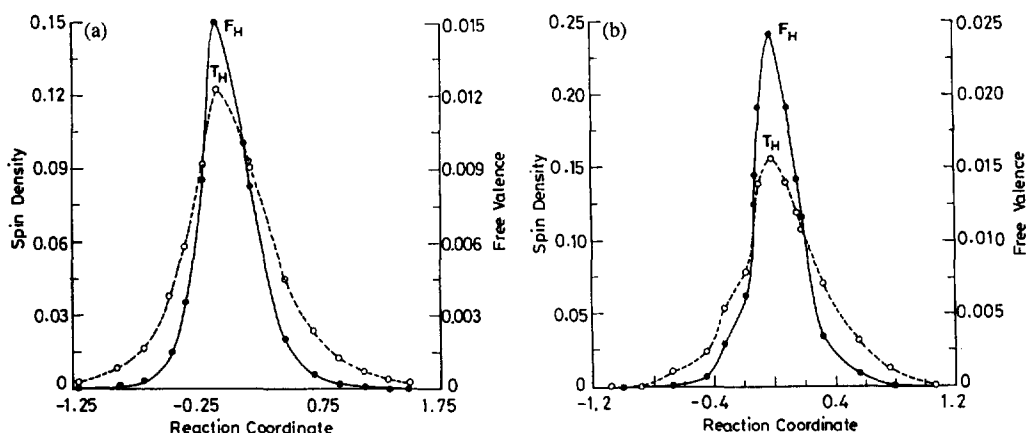


Fig. 5. Spin density (dashed lines) and free valence (solid lines) profiles of the 1:5 hydrogen transfer reactions in (a) pentane-2-one and (b) 2-methyl-1-pentene.

profiles coincide exactly with the maxima observed in the free valence (or spin density) profiles. This means that the photochemical intramolecular hydrogen abstraction by the ($^3n\pi^*$) state of a ketone and the ($^3\pi\pi^*$) state of an alkene follow the same mechanism as the hydrogen abstraction reaction by a free radical does in the radical-exchange reaction on the ground state surface.

4.3. Synchronicity in bond-formation and bond-cleavage processes

Another question which we would like to address now is whether or not the formation of the X1–H1 bond and the cleavage of the C5–H1 bond with the migrating hydrogen H1 are simultaneous during the intramolecular process. Previtali and Scaiano [30] observed that in the photochemical intramolecular hydrogen abstraction process of a ketone, the formation of the O–H bond is simultaneous with the cleavage of the C–H bond in its lowest triplet state. To obtain a more quantitative picture of the extent of transformation of differ-

ent bonds at the different stages of the same reaction, we consider here the following index χ_{AB} defined as

$$\chi_{AB} = \frac{B_{AB} - B_{AB}^i}{B_{AB}^f - B_{AB}^i} \quad (6)$$

where B_{AB} , B_{AB}^i and B_{AB}^f are the bond-orders of the bond AB at a given stage of the reaction, at the beginning and at the end of the reaction respectively. Lendvay [31] used this quantity to show the extent to which the transformation of the bond is completed. Initially, $\chi_{AB} = 0$ and then χ_{AB} increases gradually to unity in the end when the transformation (bond cleavage or bond formation) is complete. Fig. 6 shows the variation of χ_{X1-H1} and χ_{C5-H1} with the reaction coordinate x for the intramolecular hydrogen transfer processes in the ketone and alkene. The results reveal that the degree of formation of the X1–H1 bond is almost equal to the degree of cleavage of the C5–H1 bond in the transition states, indicated by arrows in Fig. 6. These reactions, therefore, primarily involve migration of hydrogen between the two heavy atoms and are not controlled by electron transfer.

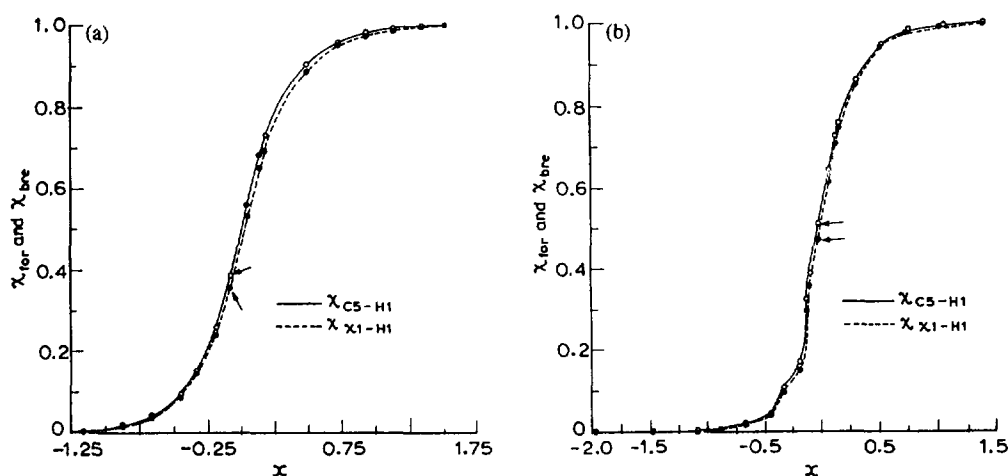


Fig. 6. χ vs. x (reaction coordinate) plots for the reaction in pentane-2-one (a) and 2-methyl-1-pentene (b). The positions of the transition states are indicated by arrows.

Wagner [27], reported that the triplet ketone abstracts hydrogen from alkyl benzene by a charge-transfer mechanism. This conclusion was based on the observation of a small isotope effect. In intramolecular hydrogen migration reactions of substituted cyclopropanes, the observed isotopic ratio k_H/k_D is small and equal to 3.0 [9]. It is believed that the primary step in the reaction is an electron-transfer rather than one-step hydrogen transfer [32].

4.4. Role of tunneling of hydrogen

There are several theoretical studies [33–35] of hydrogen tunneling on the ground state surface. Recently, we [16] reported a study on hydrogen-tunneling in photo-enolization of a ketone which involves intramolecular 1:5 hydrogen transfer. Our study, along with the experimental works of Grellmann et al. [12], reveals that tunneling is very significant in the enolization process in the temperature range 80–350 K. The present calculations lead to saddle point imaginary frequencies greater than $2000i \text{ cm}^{-1}$ for both the intramolecular hydrogen transfer processes. The imaginary frequency governs the width of the barrier and has a significant effect on the tunneling dynamics. The associated eigenvector has a large component of hydrogenic motion. Thus, one expects tunneling to be important in the intramolecular γ -hydrogen transfer reactions of ketone and alkene. To determine the role of tunneling of hydrogen in these processes, we follow the same procedure as described in earlier papers [16,36].

To calculate the probability of hydrogen tunneling, we fit the theoretically calculated MEP (Fig. 3) with the following polynomial function

$$V(x-x_0) = V_0 + \sum_{i=1}^7 l_i (x-x_0)^i \quad (7)$$

where x_0 is the value of the reaction coordinate at the transition state and V_0 is the energy barrier for the reaction. The coefficients l_i in Eq. (7), are constants with appropriate dimensions. The above polynomial fits reasonably well with the theoretically computed one-dimensional energy profiles. A similar polynomial, but of lower order, was used earlier [16] to fit the potential energy profile of the keto-enol tautomerism on its lowest triplet state.

To calculate the probability $P(E)$ of hydrogen tunneling, we used the WKB method of approximation [37]. $P(E)$ is given by

$$P(E) = \exp \left[-2 \left(\frac{8\pi^2 \mu}{h^2} \int_a^b (V(x) - E) \right)^{1/2} dx \right] \quad (8)$$

where $V(x)$ is the potential function given by Eq. (7), E is the energy of the tunneling particle, μ is the reduced mass, $(b-a)$ is the tunneling distance which depends on the energy E according to Fig. 3, and h is Planck's constant. The above integral in Eq. (8) is obtained by numerical integration. The

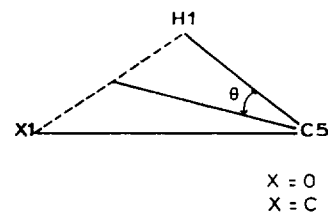


Fig. 7. The non-linear structure of X1–H1–C5 where the angle θ is defined.

specific unimolecular rate constant for the 1:5 hydrogen transfer process $k(E)$ may be given by the product of the frequency factor ν_{eff} , where ν_{eff} is the effective frequency, and the barrier permeability $P(E)$, i.e. $K(E) = \nu_{\text{eff}} P(E)$.

During the 1:5 hydrogen transfer in ketone and alkene, the migrating hydrogen atom moves along a path which, in general, does not correspond to any specific normal mode of the reactant. The hydrogen transfer involves not only the stretching motion of the C5–H1 bond but also the bending motion of H1–C5–C4 (Fig. 1). The two harmonic degrees of freedom have been converted into one effective degree of freedom with frequency ν_{eff} , which may be given as

$$\nu_{\text{eff}} = \nu_{\text{str}} \cos^2 \theta + \nu_{\text{bend}} \sin^2 \theta \quad (9)$$

where ν_{str} and ν_{bend} are the C5–H1 stretching and bending frequencies respectively, and θ is the angle between the C5–H1 bond and the line connecting C5 with the midpoint of the tunneling path in the reactant (Fig. 7). Since the optimized structures of the reactants (ketone and alkene) are known, the value of θ for ketone is estimated at 31° while for alkene it is 43.5° . Isotopic substitution for the migrating atom changes ν_{str} and ν_{bend} but not θ or any bond distances. A similar treatment was used earlier by Siebrand et al. [38] to calculate the effective frequency of a non-linear triatomic system. We calculated the effective frequencies from the AM1 frequencies for ketone and alkene. The $\nu_{\text{eff}}^{\text{H}}$ and $\nu_{\text{eff}}^{\text{D}}$ for ketone are 2543 cm^{-1} and 1858 cm^{-1} respectively, and for the alkene 2156 cm^{-1} and 1584 cm^{-1} respectively.

We then take a thermal average of the specific rate constant at a given temperature T . It is known that the temperature-dependence of the tunneling rate constant is caused by thermally activated tunneling. To describe the transition from temperature-dependent to temperature-independent tunneling, one should assume that not only the high frequency stretching and bending modes are active, but also the low frequency vibrational as well as the rotational modes. We considered eight and nine low frequency vibrational modes that are observed within the range 44 cm^{-1} – 500 cm^{-1} in the case of pentane-2-one and 2-methyl-1-pentene respectively. In addition, we included the three rotational modes which are expected to be populated even at low temperatures giving rise to slight temperature-dependent rate constants at low temperatures. The thermally averaged rate constant at a given temperature T is given by

$$k(T) = \nu_{\text{eff}} \frac{\sum_{v_1} \sum_{v_2} \dots \sum_{j_1} \dots \sum_{j_3} P(E_{v_r}) \exp(-E_{v_r}/K_b T)}{\sum_{v_1} \sum_{v_2} \dots \sum_{j_1} \dots \sum_{j_3} \exp(-E_{v_r}/K_b T)} \quad (10)$$

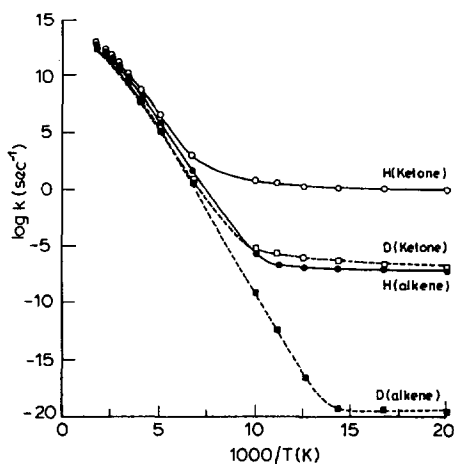


Fig. 8. The plots of $\log k_{\text{H}}$ (or $\log k_{\text{D}}$) vs. $1000/T$. The solid lines refer to H-transfer and the dashed lines refer to D-transfer in pentane-2-one and 2-methyl-1-pentene respectively.

where ν and j are the low frequency vibrational and three rotational modes respectively, and K_{b} is the Boltzmann constant. E_{vr} is the rotational-vibrational energy of the reactant and is given by

$$E_{\text{vr}} = E_{\text{ZPE}} + \nu_1 h \nu_1 + \nu_2 h \nu_2 + \dots + \sum_{i=1}^3 j_i(j_i + 1) B_i \quad (11)$$

where E_{ZPE} is the total zero-point energy of the system and B_i is a rotational constant. Since E_{vr} consists of rotational as well as low frequency modes, it will be a reasonable approximation to replace the summation by integration in Eq. (10). In other words, the energy spectrum of the low-frequency vibrational and rotational modes are assumed to be continuous. Hence, we write

$$k(T) = \nu_{\text{eff}} \frac{\int_{E_{\text{ZPE}}}^{\alpha} N(E'_{\text{vr}}) P(E_{\text{vr}}) \exp(-E'_{\text{vr}}/K_{\text{b}}T)}{\int_{E_{\text{ZPE}}}^{\alpha} P(E_{\text{vr}}) \exp(-E'_{\text{vr}}/K_{\text{b}}T)} \quad (12)$$

where $E'_{\text{vr}} = E_{\text{vr}} - E_{\text{ZPE}}$ and $N(E'_{\text{vr}})$ is the density of states at a non-fixed energy E'_{vr} which has been calculated using the Whitten–Rabinovitch approximation [39]. The density of states $N(E'_{\text{vr}})$ is higher when the migrating hydrogen is substituted by deuterium.

The plots of $\log k_{\text{H}}$ (k_{D}) vs. $1000/T$ are displayed in Fig. 8 for the ketone and alkene. Fig. 8 reveals that, below 100 K, the rate constants of the hydrogen or deuterium abstractions in ketone and alkene become almost temperature independent and are too slow to compete with the intersystem-crossing which is almost temperature independent and isotope independent [12]. Furthermore, Fig. 8 indicates that if we want to compare the 1:5 hydrogen transfer process in the ketone and alkene, we find that the tunneling of hydrogen is slower in alkene than in ketone in the low-temperature regions. This can be attributed to the larger width of the barrier at the base in alkene (Fig. 3) than in the corresponding ketone. Fig. 8 gives an apparent linear plot of $\log k_{\text{H}}$ (or $\log k_{\text{D}}$) vs. $1000/T$ at higher temperatures for both ketone and alkene, for which the rate constants are of the same order of magnitude. The linear plot does not mean that the rate constants follow the

classical behavior. The tunneling correction is quite appreciable even at 600 K, where the tunneling factors Γ_{H} (defined as $k_{\text{H}}^{\text{Q}}/k_{\text{H}}^{\text{Ar}}$ where k_{H}^{Q} and k_{H}^{Ar} are the quantum and Arrhenius rate constants respectively) for the H-transfer process in ketone and alkene are estimated at 0.6×10^3 and 0.9×10^3 respectively. The tunnel effect mechanism as such does not lead to deviations from the linear Arrhenius plot at high temperatures. A similar observation was made earlier by Weiss [40] for proton-transfer in acid–base reactions.

The calculated ratio $k_{\text{H}}/k_{\text{D}}$ for alkene at 300 K is 3.3 in agreement with the observed value for the 1:5 hydrogen transfer process in substituted cyclopropenes [9]. However, our calculated $k_{\text{H}}/k_{\text{D}}$ for the similar process in ketone is 7.0 at 300 K. No experimental data are available for the intramolecular process in ketone. If the γ -hydrogen abstraction is the main deactivation mechanism at room temperature, a kinetic isotope effect of approximately 6–8 is expected [41]. The low value of the isotope effect in these hydrogen transfer processes does not mean that an electron-transfer mechanism operates. The tunneling factors Γ_{H} and Γ_{D} for the H- and D-transfer processes respectively are very high and almost cancel out in the ratio $k_{\text{H}}/k_{\text{D}}$. For example, at 300 K, Γ_{H} and Γ_{D} for ketone and alkene are of the order of 10^4 . Our results, therefore, indicate that the intramolecular 1:5 hydrogen (or deuterium) transfer process occurs primarily via tunneling even at high temperatures. The failure to observe the Norrish type II process in alkenes might be due to their short triplet lifetimes.

5. Conclusion

An olefinic bond and a carbonyl chromophore can abstract hydrogen in their lowest triplet states by an intramolecular 1:5 hydrogen transfer process (Norrish type II). The hydrogen-transfer in the ($^3n\pi^*$) state of a ketone is exothermic while in the ($^3\pi\pi^*$) state of an alkene the process is almost thermoneutral. In both ketone and alkene, in their lowest triplet states, the abstracting atom develops a large free valence as in a free radical and therefore abstracts hydrogen as in radical-exchange reaction which occurs on the ground state surface. The photochemical intramolecular reactions involve primarily migration of hydrogen between two heavy atoms where the formation of a new bond and the cleavage of the old bond with the common migrating hydrogen atom are almost synchronous. There is no evidence of operation of an electron-transfer mechanism controlling the hydrogen-transfer process. The tunneling of hydrogen plays an important role in the hydrogen transfer process even though the isotopic ratio $k_{\text{H}}/k_{\text{D}}$ is small at room temperature.

Acknowledgements

One of the authors (AKC) is grateful to CSIR (Government of India) for financial support.

References

- [1] N.C. Yang and D.H. Yang, *J. Am. Chem. Soc.*, **80** (1958) 2931.
- [2] P.J. Wagner, *Acc. Chem. Res.*, **4** (1971) 168.
- [3] D. Sengupta, R. Sumathi and A.K. Chandra, *J. Photochem. Photobiol., A: Chem.*, **60** (1991) 149.
- [4] H.M. Rosenberg and P. Serve, *J. Am. Chem. Soc.*, **92** (1970) 4746.
- [5] J.M. Hornback, *J. Am. Chem. Soc.*, **96** (1974) 6773.
- [6] T.S. Cantrell, *Chem. Commun.*, (1970) 1633.
- [7] F. Scully and H. Morrison, *J. Chem. Soc. Chem. Commun.*, (1973) 529.
- [8] A. Padwa, U. Chiaccho and N. Hatanaka, *J. Am. Chem. Soc.*, **100** (1978) 3928.
- [9] A. Padwa and L.W. Terry, *J. Org. Chem.*, **51** (1986) 3738.
- [10] R.W. Yip and W. Siebrand, *Chem. Phys. Lett.*, **13** (1972) 209.
- [11] K.H. Grellmann, H. Weller and E. Taur, *Chem. Phys. Lett.*, **95** (1983) 195.
- [12] W. Al-Soufi, A. Eychmaller and K.H. Grellmann, *J. Phys. Chem.*, **95** (1991) 2022.
- [13] M. A. Garcia-Garibay, A. Gamarnik, L. Pang and W.S. Jenks, *J. Am. Chem. Soc.*, **116** (1994) 12095.
- [14] M.V. Encina and E.A. Lissi, *J. Photochem.*, **6** (1976) 173.
- [15] P.J. Wagner, P.A. Kelso and R.G. Zepp, *J. Am. Chem. Soc.*, **94** (1972) 7480.
- [16] D. Sengupta and A.K. Chandra, *Int. J. Quantum Chem.*, **52** (1994) 1317.
- [17] J.R. Scheffer, *Org. Photochem.*, **8** (1987) 249.
- [18] D. Sengupta and A.K. Chandra, *J. Photochem. Photobiol., A: Chem.*, **73** (1993) 151.
- [19] D. Sengupta, A. Bhattacharya, R. Sumathi and A.K. Chandra, *J. Photochem. Photobiol., A: Chem.*, **86** (1995) 161.
- [20] M.J.S. Dewar, E.G. Zoebish, E.F. Healy and J.J.P. Stewart, *J. Am. Chem. Soc.*, **107** (1985) 3902.
- [21] M.J.S. Dewar, E.G. Zoebish, E.F. Healy and J.J.P. Stewart, *Quantum Chemistry Program Exchange Package No. 455*, 1985.
- [22] I. Mayer, *Chem. Phys. Lett.*, **97** (1983) 210.
- [23] I. Mayer, *Int. J. Quantum Chem.*, **29** (1986) 73.
- [24] I. Mayer, *Int. J. Quantum Chem.*, **29** (1986) 477.
- [25] V. Sreedhara Rao, D. Sengupta and A.K. Chandra, *J. Mol. Struct. (Theochem)* **361** (1996) 151–160.
- [26] P.J. Wagner and G.S. Hammond, *J. Am. Chem. Soc.*, **88** (1966) 1245.
- [27] P.J. Wagner, *Top. Curr. Chem.*, **66** (1976) 1–52.
- [28] R. Daudel, C. Leroy, D. Peters and M. Sana, *Quantum Chemistry*, Wiley, New York, 1983, Chapter 6.
- [29] H.M. Rosenberg and M.P. Serve, *J. Am. Chem. Soc.*, **92** (1970) 141.
- [30] C.M. Previtali and J.C. Scaiano, *J. Chem. Soc., Perkin Trans. II*, (1972) 1667.
- [31] G. Lendvay, *J. Phys. Chem.*, **98** (1994) 6098.
- [32] G. Eigenman, *Helv. Chim. Acta.*, **46** (1963) 864.
- [33] A.K. Chandra, E.J.P. Malar and D. Sengupta, *Int. J. Quantum Chem.*, **41** (1992) 351.
- [34] A.K. Chandra and V.S. Rao, *Int. J. Quantum Chem.*, **47** (1993) 437.
- [35] P.D. Pacey and W. Siebrand, *Can. J. Chem.*, **66** (1988) 875.
- [36] M.T. Nguyen, D. Sengupta and L.G. Vanquickenborne, *Chem. Phys. Lett.*, **244** (1995) 83.
- [37] D. Park, *Introduction to Quantum Theory*, McGraw Hill, New York, 1974.
- [38] W. Siebrand, T.A. Wildman and M.Z. Zgierski, *J. Am. Chem. Soc.*, **106** (1984) 4089.
- [39] G.Z. Whitten and B.S. Rabinovitch, *J. Chem. Phys.*, **38** (1963) 2466.
- [40] J.J. Weiss, *J. Chem. Phys.*, **41** (1964) 1120.
- [41] N.S. Isaacs, *Physical Organic Chemistry*, Wiley, New York, 1987, Chapter 7.